Materials Research. 2025; 28(suppl. 1): e20250025
DOI: https://doi.org/10.1590/1980-5373-MR-2025-0025

Characterization of Structural Mortars Reinforced with Sisal Fibre, Recycled Rubber and Expanded Vermiculite

A.C.G. Da Silva[a*], A.G. Oliveira[a], T.G.S. Righetto[a], L.S. Batista[a], A.E. Gomes[b],

P. Serna[c], H.J.F. Diógenes[d], L.A. Gachet[a], R.C.C. Lintz[a]

[a]*Universidade Estadual de Campinas, Campinas, SP, Brasil.*
[b]*Universidade Federal de Itajubá, Itajubá, MG, Brasil.*
[c]*Universitat Politècnica de València, València, Comunidad Valenciana, Espanha.*
[d]*Universidade Federal da Paraíba, João Pessoa, PB, Brasil.*

Received: January 14, 2025; Revised: July 14, 2025; Accepted: August 14, 2025

The construction of cisterns — reservoirs specifically designed for the collection, storage, and conservation of water — has emerged as a significant strategy for mitigating water scarcity in arid regions. A widely adopted form of cistern construction involves the use of cementitious composite panels. This study investigates the mechanical properties of cementitious composites incorporating rubber waste, expanded vermiculite, and sisal fibres. Three distinct mortar formulations were developed and evaluated in terms of water absorption, voids index, specific mass, compressive strength, flexural tensile strength, dynamic modulus of elasticity, and damping factor. Relative to the reference mixture, the incorporation of sisal fibres (SF) in conjunction with rubber and vermiculite resulted in a 12–16% reduction in density, a 29.5–30.4% decrease in the dynamic modulus of elasticity, and a 2.5–9.0% increase in the damping factor. Despite an observed reduction of approximately 40% in compressive strength, the values remained within the acceptable range for structural applications. These findings substantiate the technical viability and environmental benefits of the proposed mortars for the sustainable construction of cisterns.

Keywords: *Mortars, Sisal fibres, Rubber waste, Expanded vermiculite, Cisterns.*

1. Introduction

The application of fibres as reinforcements in cementitious composites has brought significant advancements to the construction industry in recent years, offering a promising approach to mitigate crack propagation, enhance abrasion resistance, and improve the toughness of materials[1,2].

However, the use of steel and polymer fibres in these composites involves industrial processes that demand substantial resource investment, rely heavily on the extraction of natural raw materials, and result in significant greenhouse gas emissions during manufacturing[3,4].

In an effort to address the sustainability challenges faced by the sector, researchers have increasingly focused on the use of natural fibres in cementitious composites to minimise environmental impact. Fibres extracted from bamboo, vine, jute, flax, and cotton have demonstrated potential for such applications[5,6]. In Brazil, a traditional construction method widely practised in the Northeast region is the taipa de pilão technique, which employs plant fibres, clay, water, and a binder.

Among various natural fibres, sisal — a fibre extracted from the leaf of the Agave sisalana species — popularly known as the "green gold of the semi-arid", stands out due to its versatility and abundance. In 2023, the Brazilian agro-industry, particularly in the Northeast region, became the world's largest producer of sisal, as depicted in Figure 1[7]. Originating from Central America, sisal is a biodegradable material with widespread applications in the automotive, naval, and textile industries[8,9]. Sisal fibre possesses favourable mechanical properties, such as modulus of elasticity, tensile strength, and toughness, making it an attractive alternative for incorporation into cementitious composites[10,11].

Despite these advantages, the interaction between natural fibres and the cementitious matrix presents some significant challenges. The alkaline environment resulting from cement hydration reactions can degrade the main components of the fibres — cellulose, hemicellulose, and lignin — compromising their incorporation into the composite[8,12]. To improve this interaction and mitigate degradation, several treatments have been applied, such as mercerisation, acetylation, isocyanate treatment, and alkaline immersion. However, some of these techniques introduce new environmental impacts, increase production costs, and may adversely alter the fibres' characteristics[8,10,13].

Ferreira et al.[14] subjected sisal fibres to ten cycles of hornification and reported an approximate 30% reduction in water absorption, a 5.2% increase in direct tensile strength, and an 8.7% decrease in modulus of elasticity.

*e-mail: augustocgomesdasilva@gmail.com
Associate Editor: Eliana Muccillo.
Editor-in-Chief: Luiz Antonio Pessan.

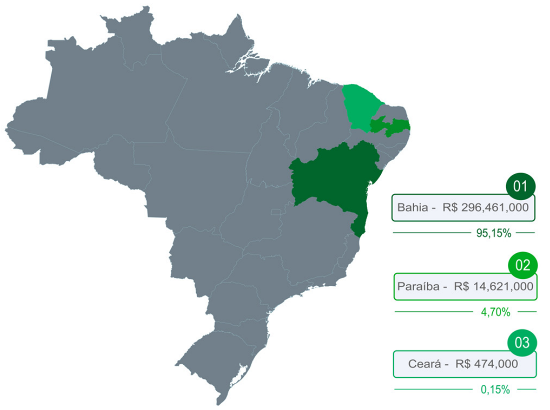

Figure 1. Map depicting the distribution and production value of sisal fibre across Brazil, adapted from 2024 data provided by the Brazilian Institute of Geography and Statistics (IBGE).

In this study, hornification treatment was applied to the fibres, aiming to offer an environmentally sustainable alternative. This process involved successive cycles of water immersion followed by controlled oven drying. Five cycles were performed to modify the physical characteristics of the sisal fibres, particularly to reduce water absorption and improve dynamic properties when incorporated into cementitious composites.

When hornification is carried out over five to ten cycles, significant structural and chemical changes occur in the fibres, resulting in notable gains in mechanical strength and bond performance with the cementitious matrix. Therefore, hornification presents itself as an efficient alternative to enhance the durability and mechanical performance of natural fibre-reinforced cementitious composites[15-17].

As an alternative to reduce specific mass and increase the energy absorption capacity of cementitious composites, lightweight aggregates have been employed to replace natural aggregates.

Akbari et al.[18] investigated the influence of expanded vermiculite and waste tyre rubber on the properties of lightweight concrete. Increasing the rubber content in the concretes (from 0 to 20%) resulted in a reduction in specific mass, improvement in fracture energy, and enhanced material ductility.

Another benefit of using rubber in cementitious composites lies in its environmental impact reduction by minimising the volume of waste sent to landfills and decreasing the extraction of natural aggregates. Through life cycle analysis, Gravina and Xie[19] studied that the production of concrete containing rubber can reduce CO_2 emissions associated with the construction industry. Although a decrease in the modulus of elasticity occurs, proper material selection and dosage optimisation can enable the production of concretes with balanced mechanical and environmental performance[20].

Another lightweight aggregate, expanded vermiculite, is used in cementitious composites to reduce density and provide heat resistance and thermal stability. Partial replacement of natural sand with vermiculite can affect workability and mechanical properties. When substituting sand with 30% and 60% vermiculite, Mo et al.[21] observed an increase in water absorption and mortar fluidity.

In a study conducted by Naveenkumar et al.[22] on reinforced concrete beams containing vermiculite, it was found that a 5% substitution of fine aggregate with expanded vermiculite led to a reduction of up to 10% in the self-weight of the beam compared to conventional reinforced concrete beams. The ultimate load for the conventional reinforced concrete beam was 120 kN, while the beam with vermiculite achieved 140 kN.

Within this context, the primary objective of the present study was to investigate the combined incorporation of hornification-treated sisal fibres, rubber waste, and expanded vermiculite into mortars to produce composites with reduced density and improved dynamic load absorption capacity.

Through this combination of sustainable materials, an alternative composite was developed for use in cistern construction in Brazil's semi-arid region, which frequently experiences prolonged drought periods.

This incorporation strategy seeks not only to promote environmental and economic sustainability but also to optimise the physical and mechanical behaviour of cementitious composites under dynamic stresses, enhancing their damping capacity in cisterns, which, being buried or semi-buried, may be subjected to such loads due to the movement of vehicle traffic or agricultural machinery.

2. Experimental

2.1. Materials

The materials used in this study were selected based on the expected properties of the developed mortars. The composition included quartz sand, with a density of 2.66 kg/dm^3; residual rubber obtained from tire retreading process, with a density of 1.14 kg/dm^3 and particle sizes ranging between 1.18 mm and 0.6 mm; and expanded vermiculite, with a density of 0.45 kg/dm^3, used as partial replacements for sand.

Additionally, high-early-strength Portland cement (CPV – ASTM Type III), silica fume with a density of 2.20 kg/dm^3, and a polycarboxylate-based superplasticizer with a density of 1.12 kg/dm^3 were used. The superplasticizer was added at a fixed dosage of 1.5% by cement mass to adjust workability. Tap water used in the mix was sourced from the public supply network. Sisal fibres with a density of 1.393 kg/dm^3, were incorporated at dosages of 10 kg/m^3 and 20 kg/m^3. The length of the sisal fibres used was 15 mm.

The physical characteristics of the aggregates were determined using different methods. For sand, the fineness modulus and maximum grain sizes were obtained through sieve analysis. For expanded vermiculite, the method specified by ABNT NBR 11355[23] was followed. The specific mass of vermiculite was determined according to the test specified by ABNT NBR 16605[24], while the sand was tested according to ABNT NBR 16916[25].

The compositions of the mixtures developed for this study are detailed in Table 1. The nomenclature of the mixes was established based on the sequence of components: mortar (M), followed by the rubber content indicated by the letter R, the expanded vermiculite content indicated by the letters EV, and the Sisal Fibre content indicated by the letters SF. The main difference between the mixtures lies in the sisal fibre dosage, which varies between 10 and 20 kg/m^3.

2.2. Fibre treatment

To improve the adhesion of the fibres to the cementitious matrix and reduce their water absorption, as indicated in the literature, the hornification treatment was applied. This process involved alternating cycles of Fibre saturation in water (sourced from the public supply and maintained at 23°C) and drying in an oven at 80°C, the maximum temperature to preserve the structural integrity of the fibres.

According to[15], this treatment is effective in reducing water absorption by the fibres and promoting the mineralization of hydration products on their surface, thereby improving the Fibre-matrix interaction.

The detailed steps of the hornification treatment are described and organized in the flowchart illustrated in Figure 2. After the treatment was completed, the fibres were cut to a length of 15 mm for incorporation into the mortars at the specified dosages.

2.3. Mixing process

To ensure mixture homogeneity, an 18-liter capacity mixer equipped with two rotational speeds—low (140 rpm) and high (285 rpm)—was used. Initially, the dry components of the mortar (sand, expanded vermiculite, rubber residue, and silica fume) were manually pre-mixed in the mixer container. After manual homogenization, the mixer was activated at low speed, and approximately 80% of the mixing water was added to the mixture.

The remaining 20% of the water was used to dilute the admixture, facilitating the removal of any viscous material adhering to the walls of the beaker used for weighing, and was then added to the mixture.

The mixing process was divided into two timed stages. In the first stage, with the mixer operating at low speed, the fibres were gradually incorporated over four minutes. During this incorporation, the fibres were manually separated to undo entanglements, as specified in ABNT NBR 7215[26].

After the fibres were fully incorporated, the mixer speed was increased to high, and the mixture was processed for a further four minutes. To meet the additive manufacturer's recommendation, the mixtures underwent a total mixing time of fifteen minutes. At the end of this process, the mortar was considered homogeneous and ready for molding.

Table 1. Composition of the mortars (kg/m³).

Mixes	Cement	Sand	Residual Rubber	Expanded Vermiculite	Silica Fume	Water	S.P.* (%)	S.F. Index (kg/m³)
M15-0R-0EV-0SF	618.0	1236.0	0	0	123.6	278.1	1.5	0.0
M15-5R-5EV-10SF	618.0	1112.4	26.6	10.5	123.6	278.1	1.5	10.0
M15-5R-5EV-20SF	618.0	1112.4	26.6	10.5	123.6	278.1	1.5	20.0

* percentage used in relation to cement mass.

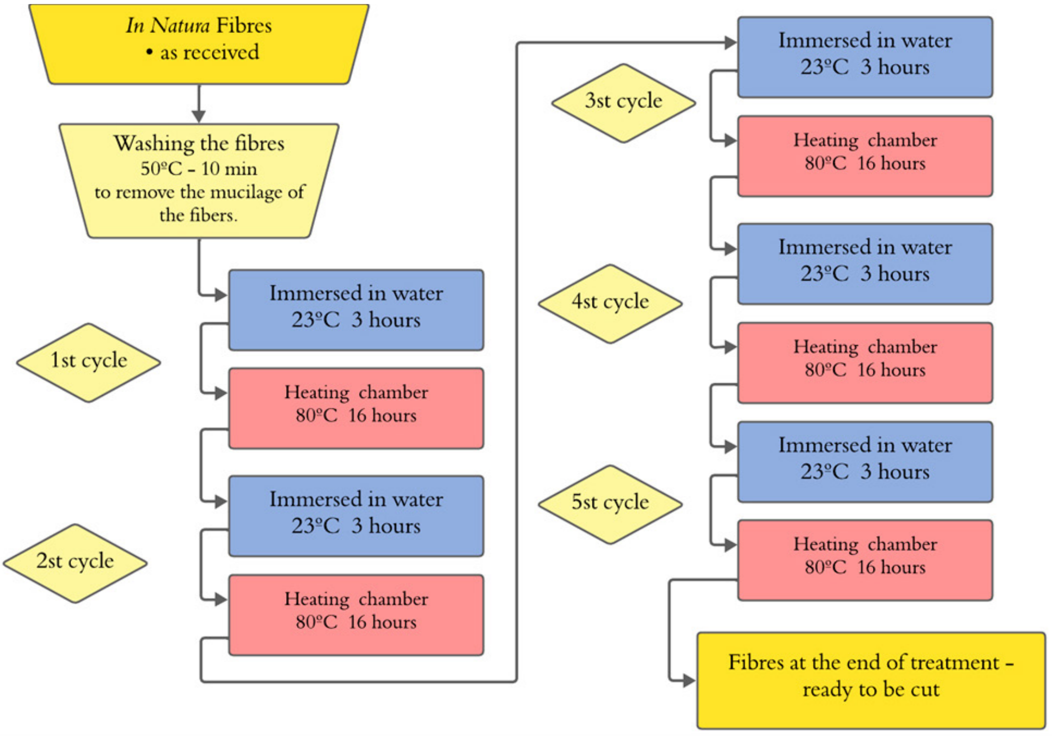

Figure 2. Flowchart of the treatment steps of the Fibre hornification method.

2.4. Specimen molding

A total of 18 prismatic specimens, with dimensions of 40x40x160 mm, and 10 cylindrical specimens, with dimensions of 50x100 mm, were molded. To facilitate demolding, the metallic molds were pre-coated with a thin layer of mineral oil and positioned with the filling opening inverted for 15 minutes to allow any excess oil to drain.

During the molding process, each mold was filled in two layers. The layers were compacted using a vibration table to eliminate air bubbles and ensure uniform distribution of the mortar within the mold.

2.5. Curing of test specimens

After 24 hours of molding, the specimens were carefully demolded and submerged in water maintained at a temperature between 20–25°C. The specimens remained in a tank located inside a humidity chamber until the specific ages for testing were reached.

2.6. Testing methods

After the mixing process, a consistency index test was conducted on the fresh mortar using the flow table method. To evaluate the mechanical and physical properties of the mortars at curing ages of 7 and 28 days, both destructive and non-destructive tests were performed.

Each mortar composition was prepared with 18 prismatic specimens (40x40x160 mm), of which 12 were allocated for destructive tests and 6 for non-destructive tests. Additionally, 10 cylindrical specimens (50x100 mm) were molded, of which 4 were used to determine specific mass, water absorption, and void index, as specified by standard ABNT NBR 9778[27].

The flexural and compressive strength tests were performed following the guidelines in standard ABNT NBR 13279[28]. All mechanical tests were conducted using an Emic electromechanical press with a 600 kN capacity, ensuring compliance with regulatory requirements.

In the flexural tensile test, the prismatic specimens were supported at two points and subjected to a gradually increasing central load, applied at a constant rate of (50 ± 10) N/s until rupture. Flexural tensile strength was calculated using the three-point bending method, ensuring accuracy in the results, as specified in Equation 1.

$$R_t = \frac{1,5 * F_t * L}{40^3} \quad (1)$$

In this test, Rt represents the flexural tensile strength (MPa), Ft is the vertical load applied at the center of the prism (N), and L refers to the support span (mm).

During the compressive strength test, the load was applied at a constant rate of (500 ± 50) N/s until specimen failure, following the guidelines in ABNT NBR 13279[28]. The calculation was performed using Equation 2.

$$R_c = \frac{F_c}{A} \quad (2)$$

In this test, compressive strength (Rc) is expressed in megapascals (MPa) and corresponds to the ratio between the applied load (Fc) measured in newtons (N) and the cross-sectional area of the specimen. The area for the prismatic specimens, with a square cross-section of 40x40 mm, was represented in square millimetres (mm^2).

Dynamic mechanical tests were conducted in accordance with standards ASTM E1876[29], ABNT NBR 8522-2[30] to determine the dynamic modulus of elasticity and damping factor of the mortars. These parameters were obtained using the Impulse Excitation Technique (IET) with Sonelastic® equipment.

This technique involves applying a short-duration mechanical impact on a prismatic specimen, generating fundamental resonance frequencies captured by an acoustic captador, as illustrated in Figure 3.

The Sonelastic® software uses algorithms based on the Fast Fourier Transform (FFT) to analyze the frequency spectrum obtained in the test, allowing precise calculation of the dynamic modulus of elasticity.

This parameter, along with the Young modulus, shear modulus, and Poisson ratio, provides a comprehensive understanding of the material's elastic properties. Additionally, the software estimates the vibration attenuation rate, directly related to the material's damping factor.

To validate the results obtained by the Impulse Excitation Technique (IET), the ultrasound test was conducted to determine the longitudinal modulus of elasticity using ultrasonic wave propagation.

This procedure utilized the same six prismatic specimens previously tested with the IET method, as both are non-destructive methods.

Using the Agricef USLab ultrasonic equipment, the specimens were analysed at 7 and 28 days, as specified in standard ABNT NBR 15630[31]. The test recorded the time required for the ultrasonic wave to travel between the transmitting and receiving transducers.

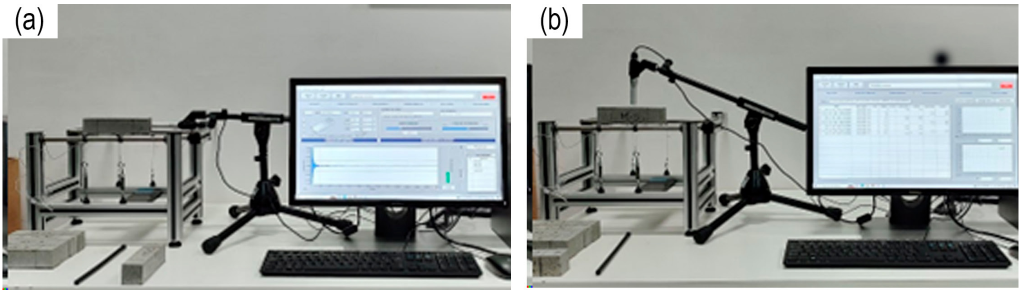

Figure 3. Sonelastic® equipment prepared for conducting the test of dynamic modulus of elasticity and damping factor in the two test reading positions: (a) longitudinal and (b) flexural.

Based on the recorded time (t, in microseconds), the ultrasonic wave propagation velocity (V) was calculated using Equation 3.

$$V = \frac{L}{t} \quad (3)$$

The length of the specimens used in the test was fixed at L = 160 mm, and the propagation velocity was obtained in mm/μs.

Using these data, along with the specimen density (ρ, in kg/m^3) and Poisson ratio (μ, assumed as 0.20), the dynamic modulus of elasticity was calculated using Equation 4.

$$E_d = V^2 * \rho * \frac{(1+\mu)*(1-(2*\mu))}{(1-\mu)} \quad (4)$$

These combined approaches allow for a detailed analysis of the dynamic behaviour of the mortars, complementing static evaluations of mechanical strength. The data obtained provide insights into structural performance over time, assisting in the development of more efficient and durable materials for dynamic applications.

3. Results

3.1. Consistency index

The results of the mortar consistency index, presented in Table 2, show a progressive decrease with the incorporation of expanded vermiculite, rubber waste, and sisal fibres.

In the mix M15-0R-0EV-10SF, compared to the reference mix, there was an 18% reduction in the consistency index. Meanwhile, increasing the Fibre content to 20 kg/m^3, as in the mix M15-0R-0EV-20SF, resulted in an even greater decrease of 24%.

This behaviour can be partially attributed to the increased amount of fibres in the mixture.

The Fibre length, set at 15 mm, proved to be more suitable for mixing compared to a length of 30 mm, as reported in the study by[32]. This configuration not only facilitated the moulding of test specimens but also the production of mesh-reinforced panels for cistern construction, preventing Fibre retention during filling and, consequently, the formation of areas with uneven material concentration.

3.2. Water absorption, specific mass, and void index

The results for water absorption, specific mass, and void index of the mortars are detailed in Table 2. It was observed that both water absorption and void index increased with higher Fibre contents in the mixture.

For the void index, increases of 21% and 34% were recorded for mixtures containing 10 kg/m^3 and 20 kg/m^3 of sisal fibres, respectively, compared to the reference mix. Regarding water absorption, the indices rose between 41% and 68%.

These increases may compromise not only the mechanical strength of the material but also its durability, as they facilitate the penetration of chloride ions and aggressive agents into the composites. These agents can expand the pores, intensify the formation of microcracks, and significantly reduce the material's service life[32,33].

However, the increase in these indices is not solely attributed to the presence of fibres. Previous studies[34] incorporating expanded vermiculite reported similar increases in the void index, even without the addition of fibres.

Regarding rubber, it was observed that due to the hydrophobic effect of its components, such as carbon black and zinc oxide (used in tire manufacturing to increase durability), it behaves as an inert material in the mixture. This characteristic promotes the formation of a well-defined transition zone between the rubber particle and the cementitious matrix, with a limited impact on water absorption[35,36].

3.3. Compressive strength and flexural tensile strength

The results of the compressive and flexural tensile strength tests performed on prismatic specimens are presented in Figures 4 and 5, respectively. For both properties, the data indicate that the increase in the void index, attributed to the presence of lightweight aggregates and sisal fibres, led to a decrease in the values obtained for the reference mix.

In compressive strength, for the mix M15-5R-5EV-10SF, containing 10% fine aggregate replacement and 10 kg/m^3 of sisal fibres, a 45% reduction in strength at 28 days was observed. However, when the Fibre content was increased to 20 kg/m^3 in the mix M15-5R-5EV-20SF, the reduction was smaller, at 42%.

This result may suggest that increasing the Fibre content contributes to load absorption by the cementitious matrix and improves crack propagation control, partially mitigating the negative effects of higher porosity.

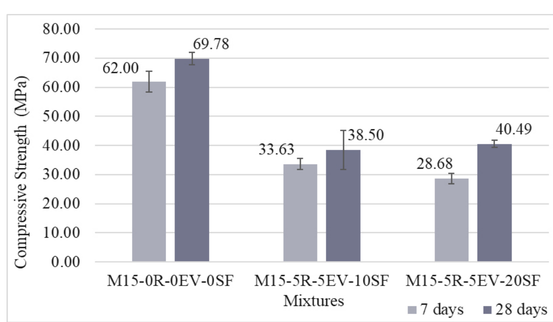

Figure 4. Results of compressive strength (MPa).

Table 2. Results of the consistency index in the fresh state of the mortars, along with water absorption, void ratio, and specific density after 28 days of curing.

Mixture	Consistency Index (cm)	Water absorption (%)	Void index (%)	Specific mass (kg/l)
M15-0R-0EV-0SF	30.60 + 0.26	5.44 + 0.21	11.53 + 0.43	2.40 + 0.01
M15-5R-5EV-10SF	25.20 + 0.17	7.63 + 0.22	13.89 + 0.30	2.11 + 0.03
M15-5R-5EV-20SF	23.37 + 0.47	9.09 +0.64	15.45 + 1.28	2.01 + 0.06

For flexural tensile strength, a 26% reduction at 28 days was observed in the mix M15-5R-5EV-10SF. However, in the mix M15-5R-5EV-20SF, the decrease was less pronounced, at only 22%.

According to the literature, authors report that for Fibre additions exceeding 3% by weight, strength properties tend to decline. This behaviour is attributed to the loss of internal load transfer capacity due to increased porosity caused by Fibre agglomeration. The most commonly cited optimal range in the literature is between 0.5% and 1% Fibre addition by weight in mortars[6,10,32,33,37,38].

3.4. Dynamic modulus of elasticity and damping factor

When analysing the dynamic properties of the material, the goal is to understand its behaviour under discontinuous load absorption, which may push the material to its strength limits. Understanding the capacity to absorb these loads and the performance limits is essential to ensure the material maintains its functionality throughout its expected service life, meeting design requirements.

The dynamic modulus of elasticity, shown in Figure 6, allows for the evaluation of both stiffness and energy dissipation capacity in vibrating systems. The technique used (IET) is non-destructive and enables the simultaneous determination of the modulus of elasticity and the damping factor.

The behaviour of the mortars concerning the dynamic modulus of elasticity follows the decreasing trend already observed in the compressive and flexural tensile strength tests. For the mix M15-5R-5EV-10SF, at 28 days, a reduction of approximately 27% was observed in both the flexural and longitudinal modulus, while the mix M15-5R-5EV-20SF showed a reduction of about 31% in both modules.

It is important to note that the main difference between the values obtained for the longitudinal and flexural moduli is related to the positioning of the microphone and the direction in which the excitation is applied to the sample during the test, since the natural vibration frequencies of the sample, in the free-free condition, are determined by the excitation of the sample through a slight mechanical impact.

Regarding the damping factor, whose results are shown in Figure 7, an increase ranging from 2.50% to 9.00% was observed with higher Fibre contents. The increase in void volume, as previously reported, facilitates the dissipation of part of the applied energy through these regions, forming barriers that aid in the absorption and dispersion of impacts.

This behaviour indicates the material's potential use in machine bases, areas near highways, or regions prone to seismic activity[39-42].

Another method for evaluating the dynamic modulus of elasticity is through the ultrasonic pulse wave method. In this process, a longitudinal wave is emitted by the transmitting transducer, travels across the distance between the rectified and opposite faces of the specimen (160 mm in length), and is captured by the receiving transducer, which records the wave's transit time from point A to point B.

The specimens were tested at 7 and 28 days, and since this is a non-destructive method, the same six specimens previously used in the IET test were employed.

The results for the longitudinal dynamic modulus obtained via the ultrasonic method are illustrated in Figure 8. Compared to the reference mix, a decreasing trend of 29.5% for the mix M15-5R-5EV-10SF and 30.4% for the mix M15-5R-5EV-20SF

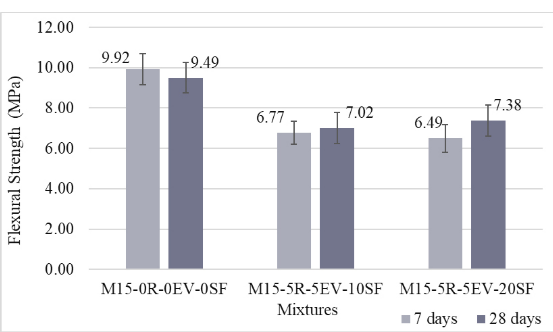

Figure 5. Results of flexural strength (MPa).

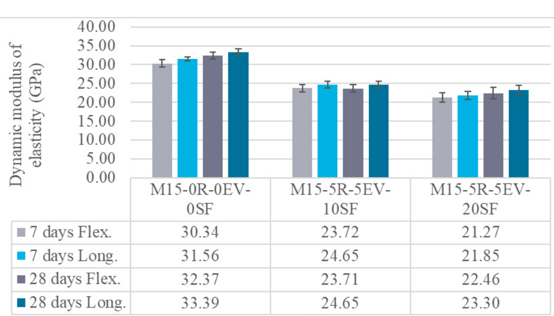

Figure 6. Results of dynamic modulus of elasticity obtained with IET (GPa).

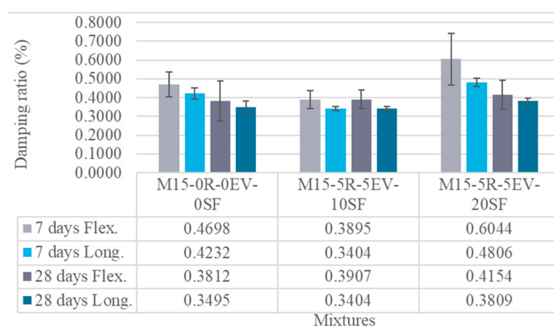

Figure 7. Results damping ratio (%).

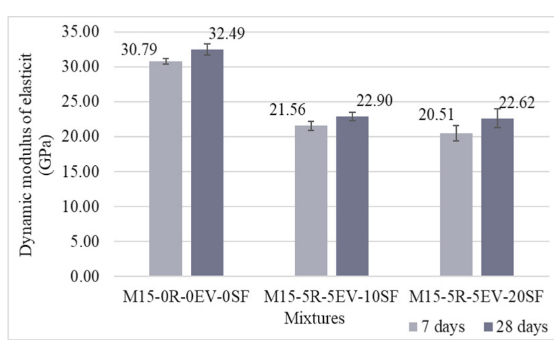

Figure 8. Results of dynamic modulus of elasticity obtained with ultrasonic pulse (GPa).

was observed a behaviour consistent with the results of the IET test, both in magnitude and proportion.

3.5. Scanning electron microscopy (SEM)

To analyse the microstructure of the mortars and the interaction between the components of the mixture, a Scanning Electron Microscopy (SEM) test was performed. Mortar fragments were collected after specimen failure, employing two distinct methodologies for sample preparation.

In the first methodology, the fragments were embedded in an acrylic resin based on polymethyl methacrylate. After resin curing, the samples underwent a sanding process with abrasive papers of varying grits until reaching an internal mortar region or a specific aggregate, enabling cross-sectional analyses.

In the second methodology, the samples were directly cut using pliers, allowing topographical analysis of the fracture surfaces.

To improve electrical conductivity and optimize image quality, the samples were coated with a thin layer of gold. Additionally, sisal fibres, both in their natural state and after the hornification treatment, were subjected to the same metallization process to analyse surface alterations. The fibre images, before and after treatment, are presented in Figure 9.

The test was conducted using the TESCAN VEGA3 scanning electron microscope, configured with a 15 kV electron beam, 500 pA current, and a 10 mm working distance. This approach enabled a detailed analysis of the microstructure of the mortars as well as the modifications induced by the treatment on the surfaces of the sisal fibres.

In the images of Figure 9(a), the natural fibre exhibits a cohesive surface characterized by the organization of cellulose microfibrils aligned and interconnected by hemicellulose, cemented by lignin. Lignin plays a fundamental role, providing structural rigidity, protection against mechanical damage, and resistance to chemical and biological agents, preserving the integrity of the fibre.

In contrast, the images in Figure 9(b) reveal significant changes in the fibre structure after the hornification treatment. During the saturation and drying cycles, partial removal of lignin occurred, along with the formation of cross-links between cellulose and hemicellulose chains.

These changes resulted in a drier, more open, and exposed surface. This structural modification facilitates fibre interaction and incorporation into the cementitious matrix, although it increases its vulnerability to degradation in alkaline environments[32,33].

Complementing these observations, Figure 9 presents analyses conducted on the mortars developed in this study. In the samples embedded in resin and polished with abrasive papers of different grit sizes, it was possible to evaluate the interfaces between the treated fibres and the cementitious matrix, providing additional insights into the implications of the treatment on the microstructure and performance of the composites.

Figures 10(a) and (b) illustrate the internal structure of the mix M15-0R-0EV-0SF, highlighting a cohesive and compact cementitious matrix. Only minor microcracks and a few dark spots, attributed to pores generated by air bubbles, are visible. These features, although present, do not compromise the overall cohesion of the matrix. These aspects support the positive strength results, indicating the efficiency of the composition in achieving a cohesive material.

On the other hand, Figures 10(c) and (d) demonstrate the impacts of incorporating materials such as sisal fibres and rubber particles into the cementitious matrix.

In Figure 10(c), the sisal Fibre exhibits a partially mineralized structure due to cement hydration reactions, confirming its interaction with the mixing water. During the curing process, the Fibre absorbed water, resulting in internal structural changes. However, the presence of lignin, which is hydrophobic in nature, formed a transition zone around the Fibre, caused by the evaporation of absorbed water released during the setting and curing of the material.

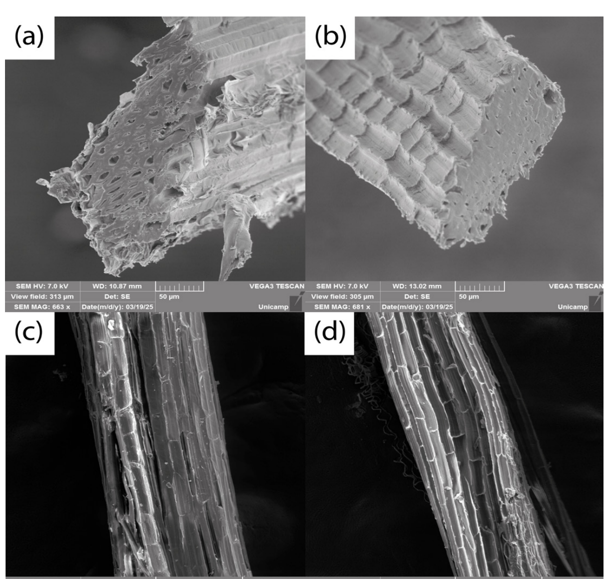

Figure 9. Microscopic analysis of fibres: In cross-sectional view (a) untreated fibre (50 µm) and (b) treated with hornification (50 µm); on longitudinal surface (c) untreated fibre (200 µm) and (d) treated with hornification (200 µm).

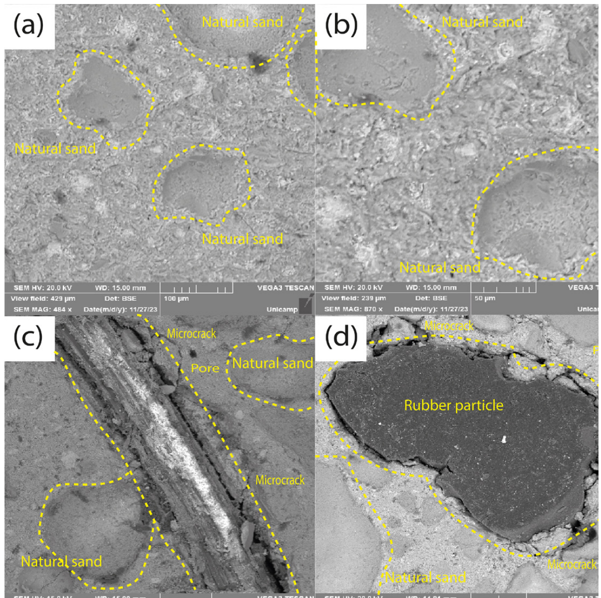

Figure 10. Microscopic analysis of resin-embedded mortars: Mix M15-0R-0EV-0SF at (a) 100 μm and (b) 50 μm; Mix M15-5R-5EV-10SF showing (c) sisal Fibre at 100 μm and (d) rubber crumb at 200 μm.

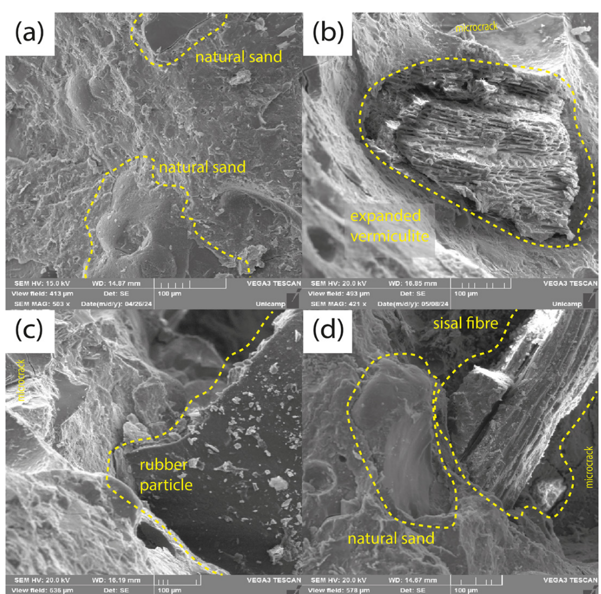

Figure 11. Microscopic analysis of post-fracture topography of mortars: Mix M15-0R-0EV-0SF at (a) 100 μm; Mix M15-5R-5EV-10SF highlighting (b) expanded vermiculite at 100 μm, (c) rubber crumb at 100 μm, and (d) sisal Fibre at 100 μm.

Meanwhile, Figure 10(d) shows a rubber particle, which also displays a transition zone around it, attributed to the material's hydrophobicity.

This characteristic, combined with the lightweight aggregates and sisal fibres, contributes to the previously reported increase in voids within the cementitious matrix. While these voids are directly associated with the reduction in mechanical strength of the composites, they play a crucial role in enhancing energy absorption capacity.

This energy is dissipated through internal friction, positively contributing to the dynamic properties of the material, such as the damping factor[43-45].

Figure 11 presents images obtained for analysing the post-failure topography of the test specimens.

In Figure 11(a), corresponding to the mix M15-0R-0EV-0SF, a more consistent microstructure is observed, in which the transition zones between the natural aggregates and the cementitious matrix are practically non-existent.

In contrast, Figure 11(b) highlights a vermiculite particle incorporated into the cementitious matrix. It is evident that the particle's structure, formed through exfoliation and expansion in a hot furnace, allows for surface interaction with the matrix. However, the deeper into the particle, the more difficult it becomes for the mortar to penetrate, resulting in higher void indices between the mineral's lamellae[34,46,47].

Figures 11(c) and 11(d) present a rubber particle and a sisal Fibre, both incorporated into the mix M15-5R-5EV-10SF.

The topographic analysis confirms previous observations: the presence of cement hydration products deposited on both the rubber particle and the sisal Fibre. However, no direct interaction between the cementitious matrix and these constituents is observed due to the previously reported formation of interfacial transition zones (ITZ)[32,33,35,40,47,48].

4. Conclusions

Based on the investigation conducted in this study regarding the physical and mechanical properties of mortars with partial replacement of fine aggregate by rubber waste and vermiculite, along with the addition of sisal fibres, and considering the analysis of the data obtained, it is possible to conclude that:

- *Fresh State of Mortars*: The incorporation of dry fibres into the composite can lead to water absorption from the mixing process by the fibres, compromising cement hydration reactions and reducing workability. This requires a higher dosage of superplasticizers, which, in turn, increases costs and demands greater financial investment.
- *Mechanical and Dynamic Properties:* Despite the reductions observed in mechanical properties—such as compressive strength (45%–42%), flexural strength (26%–22%), and dynamic modulus of elasticity (29.5%–30.4%)—the increase in the damping factor (2.5%–9.0%) indicates that the studied composite shows potential for applications requiring higher energy absorption and damping. This performance may be particularly advantageous for cisterns, the primary focus of this study, which, when buried or semi-buried, may be subjected to variable loads from nearby roads and must maintain structural integrity.
- *Fibre Durability:* The reduction in lignin content in the fibres can improve their incorporation into the cementitious matrix. However, this modification compromises Fibre durability, making them more susceptible to reactions in the alkaline matrix, potentially reducing the material's service life.
- Therefore, further studies on Fibre degradation within composites are necessary to ensure greater durability and long-term performance.

5. Acknowledgments

This study was financed in part by the Coordenação de Aperfeiçoamento de Pessoal de Nível Superior - Brasil (CAPES) - Finance Code 001, Conselho Nacional de Desenvolvimento Científico e Tecnológico (CNPq) (proc. 310375/2020-7 and proc. 309102/2023-5) and Fundação de Amparo à Pesquisa do Estado de São Paulo (FAPESP) (proc. 2022/08986-1 and proc. 21/11380-5). The authors also thank the Postgraduate Program in Technology of University of Campinas (UNICAMP).

6. References

1. Fu C, Ye H, Wang K, Zhu K, He C, et al. Evolution of mechanical properties of steel fiber-reinforced rubberized concrete (FR-RC). Compos, Part B Eng. 2019;160:158-66. http://doi.org/10.1016/j.compositesb.2018.10.045.
2. Zhang X, Lin X, Chen Y. Study on mechanical properties of steel fiber reinforced nano-concrete (SFRNC) after elevated temperature. Compos Struct. 2021;268:113941. http://doi.org/10.1016/j.compstruct.2021.113941.
3. Sbahieh S, Mckay G, Al-Ghamdi SG. A comparative life cycle assessment of fiber-reinforced polymers as a sustainable reinforcement option in concrete beams. Front Built Environ. 2023;9:1194121. http://doi.org/10.3389/fbuil.2023.1194121.
4. Nguyen W, Martinez DM, Jen G, Duncan JF, Ostertag CP. Interaction between global warming potential, durability, and structural properties of fiber-reinforced concrete with high waste materials inclusion. Resour Conserv Recycling. 2021;169:105453. http://doi.org/10.1016/j.resconrec.2021.105453.
5. Lima PRL, Toledo RD Fo, Melo JA Fo. Compressive stress-strain behaviour of cement mortar-composites reinforced with short sisal fibre. Mater Res. 2013;17(1):38-46. http://doi.org/10.1590/S1516-14392013005000181.
6. Martin AR, Martins MA, Mattoso LHC, Silva ORRF. Caracterização química e estrutural de fibra de sisal da variedade Agave sisalana. Polímeros. 2009;19(1):40-6. http://doi.org/10.1590/S0104-14282009000100011.
7. IBGE: Instituto Brasileiro de Geografia e Estatística [homepage on the Internet]. Produção agropecuária. Rio de Janeiro: IBGE; 2024 [cited 2024 Dec 14]. Available from: https://www.ibge.gov.br/explica/producao-agropecuaria/sisal-fibra/br
8. Fernandes RAP, Silveira P, Bastos B, Pereira PC, Melo V, Monteiro S, et al. Bio-based composites for light automotive parts: statistical analysis of mechanical properties; effect of matrix and alkali treatment in sisal fibers. Polymers. 2022;14(17):3566. http://doi.org/10.3390/polym14173566.
9. Chandrasekaran RG, Ramakrishna G. Experimental investigation on mechanical properties of economical local natural fibre reinforced cement mortar. Mater Today Proc. 2021;46:7633-8. http://doi.org/10.1016/j.matpr.2021.01.908.
10. Thanon Dawood E, Hani Abdullah M. Behavior of non-reinforced and reinforced green mortar with fibers. Open Eng. 2020;11(1):67-84. http://doi.org/10.1515/eng-2021-0006.
11. Martin AR, Martins MA, Mattoso LHC, Silva ORRF. Caracterização química e estrutural de fibra de sisal da variedade Agave sisalana. Polímeros. 2009;19(1):40-6. http://doi.org/10.1590/S0104-14282009000100011.
12. Wei J, Meyer C. Degradation mechanisms of natural fiber in the matrix of cement composites. Cement Concr Res. 2015;73:1-16. http://doi.org/10.1016/j.cemconres.2015.02.019.
13. Wongsa A, Kunthawatwong R, Naenudon S, Sata V, Chindaprasirt P. Natural fiber reinforced high calcium fly ash geopolymer mortar. Constr Build Mater. 2020;241:118143. http://doi.org/10.1016/j.conbuildmat.2020.118143.
14. Ferreira SR, Lima PRL, Silva FA, Toledo RD Fo. Influência de ciclos molhagem-secagem em fibras de sisal sobre a aderência com matrizes de cimento Portland. Revista Matéria. 2012;17(2):1024-34. http://doi.org/10.1590/S1517-70762012000200008.
15. Ferreira SR, Silva FA, Lima PRL, Toledo RD Fo. Effect of hornification on the structure, tensile behavior and fiber matrix bond of sisal, jute and curauá fiber cement based composite systems. Constr Build Mater. 2016;139:551-61. http://doi.org/10.1016/j.conbuildmat.2016.10.004.
16. Amaral LM, Rodrigues CS, Poggiali FJS. Hornification on vegetable fibers to improve fiber-cement composites: a critical review. J Build Eng. 2022;48:103947. http://doi.org/10.1016/j.jobe.2021.103947.
17. Ren G, Chen T, Gao X, Su A. Insights into thermal stability and interface bond performance of sisal fiber in ultra-high performance concrete under different curing conditions. Cement Concr Compos. 2023;137:104910. http://doi.org/10.1016/j.cemconcomp.2022.104910.

18. Akbari M, Tahamtan MHN, Fallah-Valukolaee S, Herozi MRZ, Shirvani MA. Investigating fracture characteristics and ductility of lightweight concrete containing crumb rubber by means of WFM and SEM methods. Theor Appl Fract Mech. 2022;117:103148. http://doi.org/10.1016/j.tafmec.2021.103148.
19. Gravina RJ, Xie T. Toward the development of sustainable concrete with Crumb Rubber: Design-oriented Models, Life-Cycle-Assessment and a site application. Constr Build Mater. 2022;315:125565. http://doi.org/10.1016/j.conbuildmat.2021.125565.
20. Cai X, Zhang L, Pan W, Wang W, Guan Q, Zhai S, et al. Study on evaluation of elastic modulus of crumb rubber concrete in meso-scale. Constr Build Mater. 2022;331:127247. http://doi.org/10.1016/j.conbuildmat.2022.127247.
21. Mo KH, Lee HJ, Liu MYJ, Ling T-C. Incorporation of expanded vermiculite lightweight aggregate in cement mortar. Constr Build Mater. 2018;179:302-6. http://doi.org/10.1016/j.conbuildmat.2018.05.219.
22. Naveenkumar K, Suriya PA, Divahar R, Sangeetha SP, Jayakumar M. Experimental investigation flexural behavior of reinforced concrete beam with partial replacement of vermiculite. Mater Today Proc. 2021;46:5885-8. http://doi.org/10.1016/j.matpr.2021.02.743.
23. ABNT: Associação Brasileira de Normas Técnicas. ABNT NBR 11355: Vermiculita expandida — Análise granulométrica — Método de ensaio. São Paulo: ABNT; 2015.
24. ABNT: Associação Brasileira de Normas Técnicas. ABNT NBR 16605: Cimento Portland e outros materiais em pó — Determinação da massa específica. São Paulo: ABNT; 2017.
25. ABNT: Associação Brasileira de Normas Técnicas. ABNT NBR 16916: Agregado miúdo - Determinação da densidade e da absorção de água. São Paulo: ABNT; 2021.
26. ABNT: Associação Brasileira de Normas Técnicas. ABNT NBR 7215: Cimento Portland — Determinação da resistência à compressão de corpos de prova cilíndricos. São Paulo: ABNT; 2019.
27. ABNT: Associação Brasileira de Normas Técnicas. ABNT NBR 9778: Argamassa e concreto endurecidos - Determinação da absorção de água, índice de vazios e massa específica. São Paulo: ABNT; 2009.
28. ABNT: Associação Brasileira de Normas Técnicas. ABNT NBR 13279: Argamassa para assentamento e revestimento de paredes e tetos - Determinação da resistência à tração na flexão e à compressão. São Paulo: ABNT; 2005.
29. ASTM: American Society for Testing and Materials. ASTM E1876: standard test method for dynamic young's modulus, shear modulus, and poisson's ratio by impulse excitation of vibration. West Conshohocken: ASTM; 2015.
30. ABNT: Associação Brasileira de Normas Técnicas. ABNT NBR 8522-2: Concreto endurecido - Determinação dos módulos de elasticidade e de deformação - Parte 2: Módulo de elasticidade dinâmico pelo método das frequências naturais de vibração. São Paulo: ABNT; 2021.
31. ABNT: Associação Brasileira de Normas Técnicas. ABNT NBR 15630: Argamassa para assentamento e revestimento de paredes e tetos - Determinação do módulo de elasticidade dinâmico através da propagação de onda ultra-sônica. São Paulo: ABNT; 2009.
32. Silva ACG, Oliveira AG, Batista LS, Gomes AE, Gachet LA, Righetto TGS, et al. Influence of the addition of sisal fibers on the physical and mechanical properties of mortars. MATEC Web Conferences. 2024;403:02007. http://doi.org/10.1051/matecconf/202440302007.
33. Amjad H, Khushnood RA, Ahmad F. Enhanced fracture and durability resilience using bio-intriggered sisal fibers in concrete. J Build Eng. 2023;76:107008. http://doi.org/10.1016/j.jobe.2023.107008.
34. García G, Cabrera R, Rolón J, Pichardo R, Thomas C. Natural fibers as reinforcement of mortar and concrete: a systematic review from Central and South American regions. J Build Eng. 2024;98:111267. http://doi.org/10.1016/j.jobe.2024.111267.
35. Dora S, Barta RB, Mini KM. Study on foam concrete incorporated with expanded vermiculite/capric acid PCM: a novel thermal storage high-performance building material. Constr Build Mater. 2023;392:131903. http://doi.org/10.1016/j.conbuildmat.2023.131903.
36. Thakare AA, Singh A, Gupta T, Chaudhary S. Effect of size variation of fibre-shaped waste tyre rubber as fine aggregate on the ductility of self-compacting concrete. Environ Sci Pollut Res Int. 2022;30(8):20031-51. http://doi.org/10.1007/s11356-022-23488-6.
37. Ince C, Shehata BMH, Derogar S, Ball RJ. Towards the development of sustainable concrete incorporating waste tyre rubbers: A long-term study of physical, mechanical & durability properties and environmental impact. J Clean Prod. 2022;334:130223. http://doi.org/10.1016/j.jclepro.2021.130223.
38. Talavera-Pech WA, Montiel-Rodríguez D, Paat-Estrella JA, López-Alcántara R, Pérez-Quiroz JT, Pérez-López T. Improvement in the carbonation resistance of construction mortar with cane bagasse fiber added. Materials. 2021;14(8):2066. http://doi.org/10.3390/ma14082066.
39. Marvila MT, Azevedo ARG, Cecchin D, Costa JM, Xavier GC, Carmo DF, et al. Durability of coating mortars containing açaí fibers. Case Studies in Construction Materials. 2020;13:e00406. http://doi.org/10.1016/j.cscm.2020.e00406.
40. Dias LS, Beserra AVS, Santos RA, Sousa AA, Lira AB No, Landim AEFG, et al. Incorporação de resíduos da produção de fibras de sisal em argamassa: efeitos nas propriedades físicas e mecânicas. Materia. 2021;26(3):e13034. http://doi.org/10.1590/s1517-707620210003.13034.
41. Bahja B, Elouafi A, Tizliouine A, Omari LH. Morphological and structural analysis of treated sisal fibers and their impact on mechanical properties in cementitious composites. J Build Eng. 2021;34:102025. http://doi.org/10.1016/j.jobe.2020.102025.
42. Liu J, Zhuge Y, Ma X, Liu M, Liu Y, Wu X, et al. Physical and mechanical properties of expanded vermiculite (EV) embedded foam concrete subjected to elevated temperatures. Case Studies in Construction Materials. 2022;16:e01038. http://doi.org/10.1016/j.cscm.2022.e01038.
43. Batista LS, Silva FM, Campos BV, Gachet LA, Santos JMC, Russo MRA, et al. Acoustic performance of concrete with rubber and vermiculite for highway barriers. Mater Res. 2023;26(Suppl. 1):e20220577. http://doi.org/10.1590/1980-5373-mr-2022-0577.
44. Moustafa A, Elgawady MA. Mechanical properties of high strength concrete with scrap tire rubber. Constr Build Mater. 2015;93:249-56. http://doi.org/10.1016/j.conbuildmat.2015.05.115.
45. Mohammed BS, Adamu M, Liew MS. Evaluating the effect of crumb rubber and nano silica on the properties of high volume fly ash roller compacted concrete pavement using non-destructive techniques. CSCM. 2018;8:380-91. http://doi.org/10.1016/j.cscm.2018.03.004.
46. Wang H, Wu Y, Cheng B. Mechanical properties of alkali-activated concrete containing crumb rubber particles. CSCM. 2022;16:e00803. http://doi.org/10.1016/j.cscm.2021.e00803.
47. Assis PC No, Sales LPB, Oliveira PKS, Silva IC, Barros IMS, Nóbrega AF, et al. Expanded vermiculite: a short review about its production, characteristics, and effects on the properties of lightweight mortars. Buildings. 2023;13(3):823. http://doi.org/10.3390/buildings13030823.
48. Silva ACG, Becker AR, Silva CTO, Marçula SC, Pereira LS, Gachet LA, et al. Comparison of the properties of mortars containing expanded clay, vermiculite, and rubber residue. Ceramica. 2023;69(392):325-31. http://doi.org/10.1590/0366-69132024703923502.

Data Availability

All data supporting the findings of this study are available upon request from the corresponding author, Augusto Carlos Gomes da Silva. The dataset is not publicly available as it forms part of a larger ongoing research project. Upon completion of the project, all data will be made publicly available in the research repository of UNICAMP.